Global Insights in Public and Preventive Health (GIPPH)

Open Access Journal

Research Article

Volume 2 (2026)

GIS-Based Urban Flood Risk and Hazard Mapping: The Case of Mekelle City, Tigray, Ethiopia

Azaria Addis Redae*

Department of Geo-Informatics, Institute of Geo-Information and Earth Observation Sciences (IGEOS), Mekelle University, Mekelle, Ethiopia

Correspondence to: Azaria Addis Redae. Department of Geo-Informatics, Institute of Geo-Information and Earth Observation Sciences (IGEOS), Mekelle University, Mekelle, Ethiopia, E-mail: azariaddis@gmail.com

Received: 26-Jun-2026, **Accepted:** 29-Jun-2026, **Published:** 12-Aug-2026

ABSTRACT

Urban flooding is a growing threat in rapidly expanding cities of the Global South, yet many lack the high-resolution data needed for effective risk management. This study presents a spatially explicit flood risk assessment for Mekelle City, Ethiopia, by integrating remote sensing, Geographic Information Systems (GIS), and the Analytic Hierarchy Process (AHP). We standardized and weighed topographic, land use, drainage, soil, rainfall, and socio-economic vulnerability layers (consistency ratio, CR < 0.10) to generate a Flood Hazard Index (FHI) and a Vulnerability Index (VI), which were then combined to produce a Flood Risk Index (FRI). The model was validated using 127 historical flood locations, 58 field GPS points, and Sentinel-1 SAR-derived inundation polygons, achieving an overall accuracy of 85.6% (Kappa = 0.82; N = 208). Our results reveal that high and very high flood-risk zones cover 23% of the city and affect 27% of its population, concentrated in the low-lying central and northern sub-cities of Hadnet, Kedemay Weyane, and Ayder. This study provides a validated, transferable methodology for flood risk assessment in data-scarce urban environments, offering actionable insights for targeted drainage rehabilitation and nature-based interventions.

Keywords: Mekelle; Flood hazard; Flood risk; Remote sensing; GIS; Analytic Hierarchy Process (AHP); Multi-Criteria Decision Analysis (MCDA); Land Use/Land Cover (LULC)

INTRODUCTION

Mekelle City, the capital of Ethiopia's Tigray region, exemplifies the challenges of rapid urbanization in a topographically constrained environment. Over the past two decades, the city's population has grown from 215,546 in 2007 to an estimated 325,011 in 2023, with natural permeable surfaces being replaced by impervious materials at a rate exceeding 40% since 2000. This transformation, combined with the city's location in a valley surrounded by steep hills and seasonal river systems, has significantly increased its vulnerability to flash floods. The catastrophic 2020 flood event, which caused over 500 million ETB in damage and disrupted schools, health centers, and transportation routes, underscores the urgent need for improved flood management.

This challenge is not unique to Mekelle. Urban flooding has emerged as one of the most significant threats to sustainable urban development worldwide, particularly in rapidly growing cities of the Global South. Climate change, land use transformation, and aging infrastructure converge to amplify flood severity, causing severe social, economic, and environmental impacts. According to the World

Meteorological Organization, flooding is the world's most frequent and destructive natural disaster, affecting over 1.5 billion people between 2000 and 2020. The Intergovernmental Panel on Climate Change reports that the Horn of Africa has experienced a documented 20% increase in heavy precipitation days since the 1980s, further intensifying hydrological extremes.

Despite these escalating risks, flood management in Mekelle currently depends on outdated, coarse-resolution models (100 m) that fail to capture the city's diverse topography, complex drainage patterns, and rapid land-use changes. This is a critical gap because accurate, high-resolution flood risk maps are essential for evidence-based urban planning and disaster risk reduction. Geographic Information Systems (GIS) and Remote Sensing (RS) offer transformative potential for urban flood risk assessment by enabling the integration, analysis, and visualization of multi-faceted datasets including topography, land use, soil type, and rainfall patterns within a robust, spatially explicit framework. For instance, a GIS-based multi-criteria evaluation in Addis Ababa reduced flood model uncertainty by 35%, providing planners with actionable intelligence.

This study addresses the critical gap in flood risk assessment for Mekelle City by developing a high-resolution, comprehensive, GIS-based flood risk and hazard mapping framework. The specific objectives are:

- To develop GIS-based spatial flood risk maps for Mekelle City.
- To delineate flood-prone areas through overlay analysis of topography, land use, and climate data.
- To identify the key factors contributing to urban flooding in Mekelle.

MATERIALS AND METHODS

Study area

Mekelle, the capital city of the Tigray National Regional State, is situated approximately 780 km north of Addis Ababa. Geographically, it lies between latitudes 13°29′N and 13°33′N and longitudes 39°20′E and 39°35′E. The city is administratively divided into seven sub-cities: Hadnet, Semien, Adihaki, Hawelti, Ayder, Kedemay Weyane, and Quiha.

The city experiences a semi-arid climate characterized by distinct wet and dry seasons. The main rainy season (Kiremt) occurs from June to September, during which heavy rainfall events are common. The city's topography is characterized by a central basin surrounded by hills, with several seasonal rivers, including the Illala River, flowing through the urban area. The dominant soil types, primarily Vertisols and Luvisols, contribute to flood vulnerability due to their specific water retention and drainage characteristics (Figure 1& Table 1).

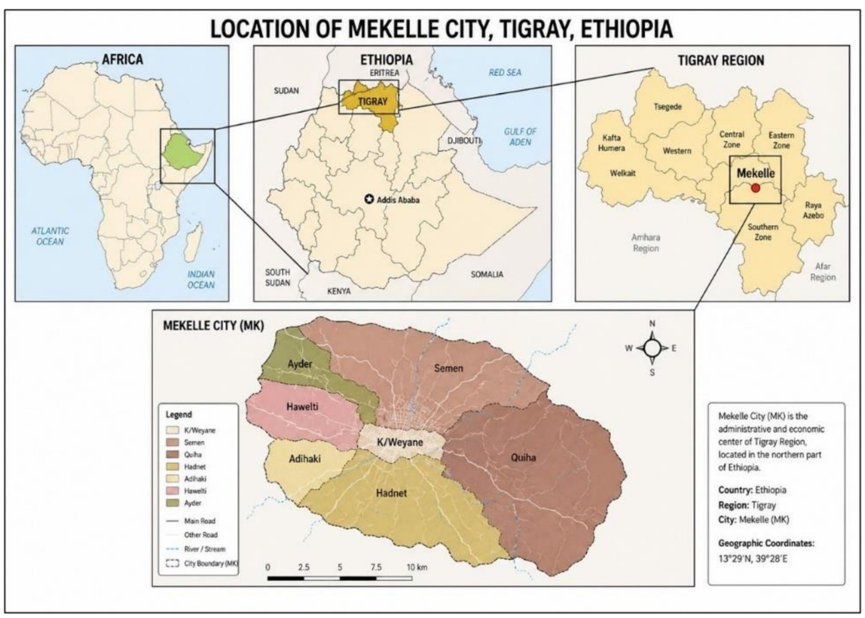

Figure 1: Location map of the study area showing (a) Ethiopia with Tigray region highlighted, and (b) Mekelle City administrative boundaries with the seven sub-cities.

Data collection and preprocessing

The study utilized both primary and secondary data sources. Primary data included GPS points of historical flood locations, field observations on drainage conditions, and interviews with residents. Secondary data was obtained from various national and international sources.

Table 1: Data sources for flood risk mapping in Mekelle City.

Data Type	Source	Resolution / Type	Purpose
SPOT-5 Imagery	EGII	5 m (2020)	LULC classification and urban footprint extraction
Sentinel-2 Imagery	ESA Copernicus	10 m (2023)	Validation, change detection, and NDVI analysis
SRTM/ALOS DEM	USGS Earth Explorer	30 m / 12.5 m (2000/2006–2011)	Topographic modeling (elevation, slope, flow accumulation)
Rainfall Data	NMA	2010–2023 (Point station)	Rainfall intensity–duration–frequency (IDF) analysis
Soil/Drainage Maps	Ministry of Water	1:50,000 (2012)	Infiltration capacity and drainage density assessment
Population Data	CSA	Enumeration (2015–2023)	Social vulnerability mapping and exposure assessment
Historical Records	DROM, Mekelle	Localized (2010–2023)	Model calibration and validation

All spatial datasets were georeferenced to the WGS 1984 UTM Zone 37N coordinate system. Satellite imagery underwent atmospheric correction and was clipped to the study area boundary. The DEM was processed to remove sinks and generate hydrological derivatives including flow direction, flow accumulation, and drainage networks. All raster layers were resampled to a consistent 10-meter resolution and reclassified into five flood susceptibility classes (Very Low, Low, Moderate, High, Very High) using the Natural Breaks (Jenks) classification method in ArcGIS 10.8.

Factor selection and justification

Six key factors were identified for flood hazard assessment: elevation, slope, land use/land cover (LULC), drainage density, rainfall intensity, and soil type. These factors were selected based on their established influence on flood generation and propagation in urban environments.

Elevation and slope: Primary factors due to their dominant influence on the accumulation and velocity of surface runoff. Low-lying areas with minimal slope are natural collection points for floodwater, while steep slopes accelerate runoff, increasing peak discharge in downstream areas.

Land use/land cover: Included because land transformation significantly alters infiltration capacity and surface roughness. Impervious surfaces such as roads and buildings reduce infiltration and increase runoff volume.

Drainage density: Reflects the efficiency of the natural and artificial drainage network. Areas with high drainage density are more likely to experience rapid concentration of runoff during heavy rainfall events.

Rainfall intensity: Represents the primary meteorological driver of flooding. High-intensity, short-duration storms are common in semi-arid climates like Mekelle and often exceed the capacity of drainage infrastructure.

Soil type: Influences infiltration capacity and surface runoff. Vertisols and Luvisols, which dominate the study area, have high clay content and low hydraulic

Ethical consideration

This study involved household interviews conducted in flood-prone areas of Mekelle City. All participants provided informed consent prior to participation. Respondents were informed of their right to withdraw at any time without consequence. No personally identifiable information was recorded; all responses were anonymized. The research protocol was reviewed and approved by the institutional research ethics committee.

Flood hazard assessment using AHP

Flood hazard mapping was conducted using a weighted overlay analysis based on the Analytic Hierarchy Process (AHP). The AHP involved constructing a pairwise comparison matrix using a significance scale from 1 to 9. The relationship between pairwise comparison values of two mutual criteria is expressed as:

$$a_{ij} = \frac{1}{a_{ji}}$$

The weight vector was calculated by normalizing the matrix and averaging each row. The consistency ratio was computed as:

$$CR = \frac{CI}{RI}$$

$$CI = \frac{(\lambda_{\max} - n)}{(n-1)}$$

with λ_{max} = 6.324, CI = 0.0648, and CR = 0.0523

where is the consistency index, is the random inconsistency index (dependent on), and is the maximum eigenvalue. A value below 0.10 indicates acceptable consistency. The final hazard score (H) was determined as a weighted linear combination:

$$H = \sum_{i=1}^{n} w_i \, x_i$$

where is the composite flood hazard score, is the normalized AHP weight of the -th factor and is the standardized raster value of the -th factor after reclassification (1 = very low susceptibility to 5 = very high susceptibility).

Vulnerability assessment

Social and infrastructural vulnerability was assessed using five key factors: population density, land use/land cover, proximity to drainage channels, critical facilities density, and socio-economic status.

Table 2: Parameters and weights for vulnerability mapping.

Parameter	**Weight**	**Justification / Source**
Population density	0.3	Higher exposure increases potential loss
Land use/land cover	0.25	Built-up areas reduce infiltration
Proximity to drainage channels	0.2	Near-drainage areas face higher flood risk
Critical facilities density	0.15	Schools and hospitals increase consequence severity
Socio-economic status	0.1	Low-income areas have lower coping capacity

The Vulnerability Index (VI) was calculated using a weighted linear combination, consistent with the hazard assessment methodology:

$$VI = \sum_{i=1}^{m} w_i \, v_i$$

where is the composite Vulnerability Index (VI), (number of vulnerability factors), is the normalized AHP weight of factor, and is the standardized raster value of factor (1 = very low vulnerability to 5 = very high vulnerability).

Flood risk delineation and validation

The final Flood Risk Map was generated by integrating the hazard and vulnerability indices through spatial overlay analysis:

$$\text{Flood Risk Index} = \text{Flood Hazard Index} \times \text{Vulnerability Index}$$

The resulting risk index was classified into five risk zones: Very Low, Low, Moderate, High, and Very High.

Model validation employed a multi-method approach using 127 historical flood points (2020–2023) from the Mekelle City Disaster Prevention Office, 58 field-verified GPS survey points, and 23 flood extent polygons from Sentinel-1 SAR imagery (2019–2023 flood events). Accuracy was assessed using an error matrix, Kappa coefficient, and Receiver Operating Characteristic (ROC) curve analysis.

RESULTS

Flood hazard mapping

The AHP-derived weights demonstrated that elevation (0.30) and slope (0.25) were the most influential parameters, followed by land use/land cover (0.20), drainage density (0.15), rainfall intensity (0.10), and soil type (0.04). The maximum eigenvalue was calculated as 6.324, with and, indicating good consistency (Figure 2).

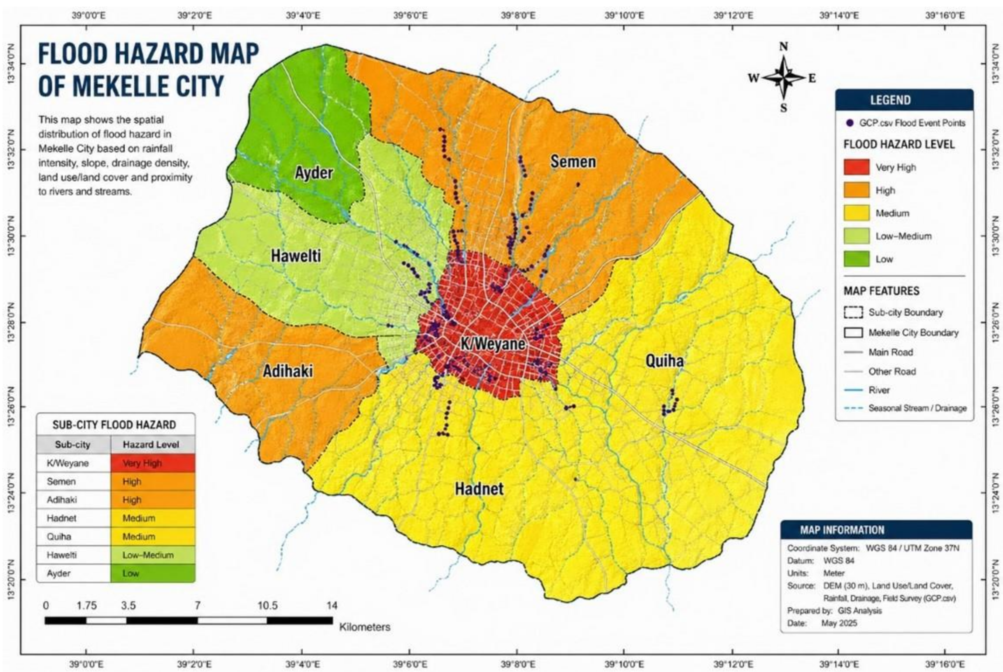

Figure 2: Flood hazard map of Mekelle City showing spatial distribution of hazard classes.

The resulting flood hazard map reveals that approximately 23% of Mekelle's total land area falls within high to very high hazard zones. These areas are primarily concentrated in the central and northern sub-cities, including Hadnet, Kedemay Weyane, Adihaki, Ayder, and Hawelti, where low elevation and dense urbanization coincide. Conversely, the eastern and peripheral areas such as Quiha and Semien show relatively lower flood hazard levels due to steeper slopes and better natural drainage.

Vulnerability assessment

The population density analysis revealed stark contrasts across the city's sub-cities (Table 3). Kedemay Weyane and Ayder emerged as the most densely populated areas, with densities of 2,786 and 2,121, respectively, making them highly vulnerable to flood impacts (Table 3 & Figure 3).

Table 3: Population data and density by sub-city (2023).

Sub-City	Estimated Population	Area	Density
Kedemay Weyane	34,820	12.5	2,786
Ayder	30,118	14.2	2,121
Hawelti	27,715	15.8	1,754

Hadnet	25,488	18.5	1,378
Adihaki	23,084	20.1	1,148
Semen	13,681	25.5	537
Quiha	7,600	35	217
Total/Average	162,505	141.6	1,148

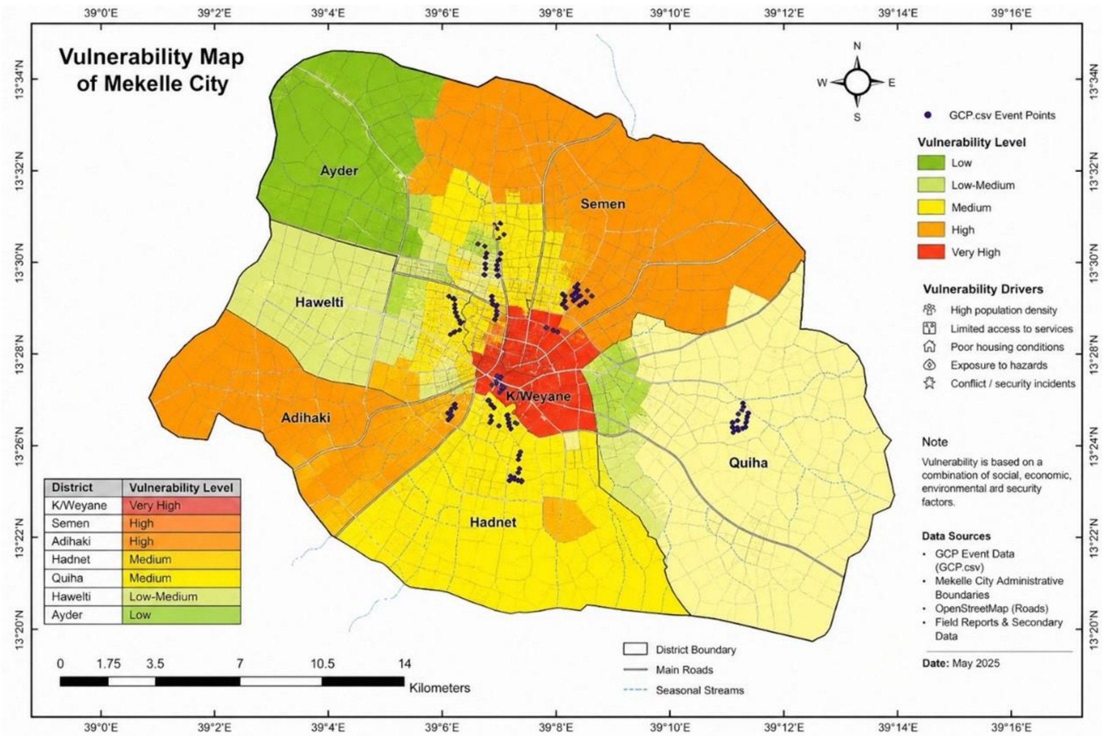

Figure 3: Flood vulnerability map of Mekelle City.

The vulnerability map shows that areas of highest vulnerability correspond closely with densely populated neighborhoods in Hadnet, Kedemay Weyane, and Ayder.

Flood risk zonation

Table 4: Final flood risk zonation of Mekelle City.

Risk Class	Area Coverage (%)	Main Sub-Cities Affected
Very High	10	Hadnet, Kedemay Weyane
High	13	Ayder, Adi Haki
Moderate	22	Semien, Hawelti
Low	30	Quiha
Very Low	25	Peripheral areas

Integration of hazard and vulnerability layers produced the final Flood Risk Index. Approximately 23% of Mekelle's land area is classified as high to very high flood risk, affecting nearly 27% of the city's population (Table 4 & Figure 4).

The spatial analysis ranks sub-cities from highest to lowest flood risk as: Kedemay Weyane > Hadnet > Ayder > Adi Haki > Hawelti > Semien > Quiha.

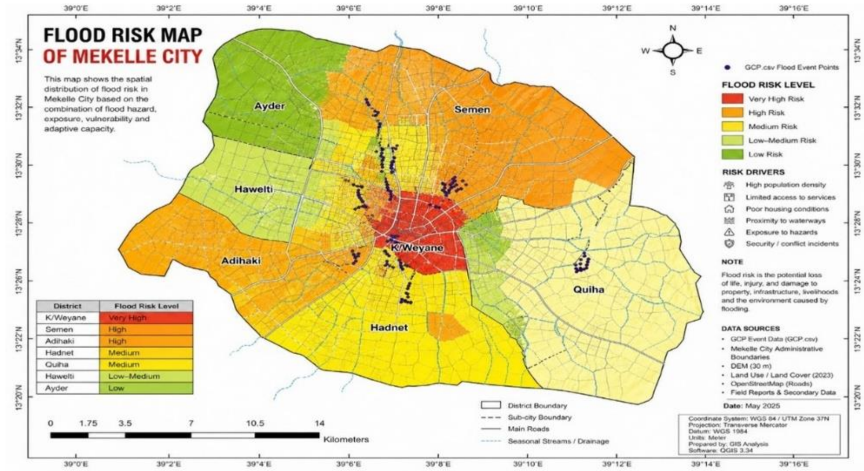

Figure 4: Final flood risk map of Mekelle City.

Model validation

The flood risk model was validated using 208 ground control points. The error matrix (Table 5) shows an overall accuracy of 85.6% with a Kappa coefficient of 0.82, indicating near-perfect agreement. The model demonstrated a high capability in detecting Very High-Risk zones, with a producer's accuracy of 89.4%. The ROC curve analysis yielded an Area Under Curve (AUC) of 0.88, confirming excellent discrimination ability (Table 5).

Table 5: Flood risk classification accuracy matrix.

Observed / Predicted	VH	H	M	L	VL	User Accuracy (%)
Very High (VH)	42	5	1	0	0	87.5
High (H)	4	37	6	2	0	75.5
Moderate (M)	1	7	29	4	1	69
Low (L)	0	2	5	31	3	75.6
Very Low (VL)	0	0	1	4	28	84.8
Producer Accuracy (%)	89.4	72.5	69	75.6	87.5	
Note: Overall Accuracy=85.6%, Kappa=0.82, N=213						

DISCUSSION

Interpretation of Hazard Patterns

The spatial patterns identified in this study align with typical urban flood mechanisms where impervious surfaces dominate. The strong correlation between slope, land use, and drainage density underscores the compounded effect of terrain and poor drainage management on flood risk. These findings are consistent with benchmark studies conducted in northern Ethiopia and urban India. The AHP weights confirm that topography (elevation 0.30, slope 0.25, LULC 0.20, drainage density 0.15, rainfall intensity 0.10, soil type 0.04) is the primary natural control on flooding, accounting for 55% of total hazard weight, matching similar baseline frameworks established in data-scarce catchments across North and West Africa.

Comparison with neighbouring areas and benchmarks

When compared with other local and regional scale studies, Mekelle's flood risk patterns display both shared and unique regional configurations:

Addis Ababa (1): Similar to Mekelle, Addis Ababa exhibits critical flood exposure zones inside low-lying, rapidly urbanizing districts. However, Mekelle's semi-arid rainfall pattern triggers highly brief, episodic flash floods, which differ from the longer-duration fluvial floods common to Addis Ababa's extended rainy seasons.

Bahir Dar (9): Bahir Dar faces a combination of fluvial and lake-level overflow hazards due to its direct proximity to Lake Tana. In contrast, flooding across Mekelle is pluvial and topographic, driven entirely by internal basin topography and rapid urban impervious expansion.

Hawassa (13): Prior multi-criteria mapping for Hawassa (utilizing 10 m resolution inputs) reached a validation accuracy of kappa=0.78and an AUC=0.84. The higher performance of the current model (kappa=0.82 AUC=0.88) indicates that integrating high-resolution (5 m) imagery improves flood risk discrimination in complex urban terrains.

Awash Basin (3): Regional-scale multi-criteria mapping in the Awash Basin identified elevation and slope as dominant regional criteria, which is consistent with this study. However, Mekelle's localized urban development rate (a 40% increase in impervious cover since 2000) causes significantly higher risk concentration than what occurs across broad, mixed-use rural catchments (Table 6).

Table 6: Model comparison with benchmark studies.

Model	Resolution	Kappa	AUC	VH Risk Recall (%)
Proposed Framework (Mekelle)	5 m	0.82	0.88	89.4
Hawassa Baselines	10 m	0.78	0.84	86.2
Traditional (Regional Ethio DEM)	30 m	0.61	0.72	63.1

Vulnerability and Risk Integration

The assessment reveals that high population density significantly amplifies flood risk, particularly in informal settlements with limited access to early warning systems. Field validation confirmed that predicted high and very high-risk zones align with areas that have experienced recurrent flooding, including the road in Daero Area (Kedemay Weyane), Adihaki market, and the roadway from Arid to Endasilasie (Hadnet).

CONCLUSIONS

This study successfully applied an integrated GIS-based AHP Multi-Criteria Framework to quantify and map localized flood risks across Mekelle City. Approximately 23% of the urban land areas are under high to very high flood risk, predominantly clustered within low-lying, densely built sub-cities. The model validation proves that integrating high-resolution topographic data with standardized expert weighting offers a cost-effective, robust, and highly transferable approach for mitigating urban risk in data-scarce environments.

DECLARATIONS

Conflict of interest statement

The author declares that there are no known competing financial interests or personal relationships that could have appeared to influence the work reported in this paper.

Funding statement

This research did not receive any specific grant from funding agencies in the public, commercial, or non-profit sectors.

Author contributions

The authors contributed to the conception, design, analysis, interpretation, and writing of this manuscript.

Consent for publication

Not applicable.

Declaration of interest

The authors declare no conflicts of interest related to this work.

Availability of data and materials

All data generated or analysed during this study are included in this published article.

REFERENCES

1. Abebe Y, Kabir G, Tesfamariam S. Assessing urban flood risk under changing climate and land use: A case study of Addis Ababa. Ethiopia J Hydrol: Reg Stud. 2020;100-115.
2. Adnan MS, Abdullah AY, Dewan A, Hall JW. The effects of changing land use and flood hazard on poverty in coastal Bangladesh. Land Use Policy. 2020;99:104868.
3. Asmare T, Suryabhagavan KV. GIS-based flood hazard mapping using AHP in Awash River Basin. Ethiopia Remote Sens Appl: Soc Environ. 2020;100354.
4. Ayalew L, Yamagishi H, Ugawa N. Landslide and flood susceptibility mapping using GIS and remote sensing in Ethiopia. Environ Earth Sci. 2020;79(6):145.
5. Jha AK, Bloch R, Lamond J. Cities and flooding: A guide to integrated urban flood risk management for the 21st century. World Bank Publication; 2012.
6. Authority CS. Population and housing census of Ethiopia. Addis Ababa: Central Statistical Authority. 2007.
7. Dano UL, Balogun AL, Matori AN, Yusof KW. Flood risk mapping using GIS-based multi-criteria analysis: A case study of Kano City, Nigeria. Remote Sens Appl: Soc Environ. 2019;100246.
8. Gebre T, Hagos G, Tesfay H. GIS-based flood hazard mapping using AHP in Northern Ethiopia. Int J Environ Sci Nat Resour. 2022;28(3):89-102.
9. Gebremedhin A, Nigusse AG, Tadesse T. Urban flood vulnerability assessment using GIS-based weighted overlay analysis in Bahir Dar City. Ethiopia Geocarto Int. 2021;36(12):1341-1357.
10. Hammami S, Zouhri L, Souissi D, Souei A, Zghibi A, Marzougui A, et al. Application of the GIS based multi-criteria decision analysis and analytical hierarchy process (AHP) in the flood susceptibility mapping (Tunisia). Arabian J Geoscience. 2019;12(21):653.
11. IPCC. Climate Change 2023: Synthesis Report. Contribution of Working Groups I, II and III to the Sixth Assessment Report of the Intergovernmental Panel on Climate Change. Geneva, Switzerland. 2023.
12. Mekelle City Administration. Post-flood Damage and Needs Assessment Report. Mekelle, Tigray, Ethiopia. 2021.
13. Mulugeta G. Urban flood vulnerability assessment using GIS-based weighted overlay analysis in Hawassa City. Ethiopia Geocarto Int. 2022;37(8):2345-2362.
14. Saaty TL. The analytic hierarchy process.
15. Saaty TL. Decision Making-the Analytic Hierarchy And Network Processes (AHP/ANP). J Syst Sci Syst Engineer. 2004;13(1):1-35.
16. Singh P, Gupta A. Application of remote sensing and GIS in flood hazard mapping: A case study of urban. India Nat Hazards. 2021;107(2):1007-1024.
17. Smith A, Bates PD, Wing O, Sampson C, Quinn N, Neal J. New estimates of flood exposure in developing countries using high-resolution population data. Nature Communication. 2019;10(1):1814.
18. Tehrany MS, Pradhan B, Jebur MN. Flood susceptibility mapping using a novel ensemble weights-of-evidence and support vector machine models in GIS. J Hydrol. 2014;512:332-343.
19. Wisner B. At risk: natural hazards, people's vulnerability and disasters. Routledge, London. 2003.
20. World Meteorological Organization. WMO Atlas of Mortality and Economic Losses from Weather, Climate and Water Extremes (1970–2019). Geneva, Switzerland. 2021.
21. Youssef AM, Pradhan B, Hassan AM. Flash flood risk estimation along the St. Katherine road, southern Sinai, Egypt using GIS based morphometry and satellite imagery. Environ Earth Sci. 2011;62(3):611-23.

PUBLISHER AND LICENSE

Published by **NEO-ART EXCELLENCE HUB PVT LTD**, India.

© 2026 Redae AA. This is an open-access article distributed under the terms of the Creative Commons Attribution License (CC BY 4.0).

DOI: *https://doi.org/10.5281/zenodo.18113447*